Local Scour at Wide Bridge Piers

Nordila A.[1]; Thamer M. Ali[2]; Faisal A.[3]; and Badrunnisa Y.[4]

Abstract: Laboratory data for local scour depth at the size of wide piers are presented. Clear water scour tests were performed various pier widths (0.06, 0.076, 0.102, 0.14 and 0.165 m), two type of pier shapes (circular and rectangular) and two types of uniform cohesionless bed sediment (d_{50} = 0.23 and d_{50} = 0.80 mm). New data are presented and used to demonstrate the effects of pier width, pier shape and sediment size on scour depth. The influence of equilibrium time (t_e) on scouring processes also discussed. Equilibrium scour depths were found to decrease with increasing values of b/d_{50}. The temporal development of equilibrium local scour depth with new laboratory data is demonstrated for flow intensity V/V_c = 0.95. On the other hand, the result of scour mechanism have shown a significant relationship between normalized volume of scoured and deposited with pier width, b. The experimental data obtained in this study and data available from the literature for wide piers are used to evaluate predictions of existing methods.

Keywords: Scour; Wide piers; Cohesionless Sediment; Equilibrium time; Scour mechanism

Introduction

Estimation of local scour depth at wide piers have been made by many researchers (e.g., Johnson and Torrico 1994; Sheppard et al 1995; Ettema et al 1998; Johnson 1999; Jones and Sheppard 2000; Sheppard et al 2004; Sheppard and Melville 2011). The wide pier scour problems have been long recognized by engineers where these problems are tend to over-predict scour depths. Several studies (Melville and Sutherland 1988; Melville and Coleman 2000) have found that the relation between the depth of local scour at a bridge pier are depends on three dimensionless groups which are (1) flow intensity (upstream depth averaged velocity divided by the sediment critical depth averaged velocity) V/V_c; (2) aspect ratio (water depth divided by pier width) y/b; and (3) pier width divided by the median sediment grain size b/d_{50}. Many of these groups such as the ratio of water depth to structure width can be maintained constant between laboratory model and prototype structure. However, major differences in the values of b/d_{50} in most laboratory and field situations. This can give a great impact on scour depth predictions at prototype scale structures especially when the structures are located in fine sand. In fact, if the b/d_{50} is not properly accounted for in the predictive equations then problems occur when the equations are applied to situations different from the laboratory conditions on which they are based (Jones and Sheppard, 2000). The engineers have long recognized this problem and it is called as "wide pier scour problem". However, most of the wide pier laboratory data reported in the literature was studied only for one type of pier shape, especially on circular pier (Garde and Kothyari 1998; Sheppard et al 1995; Sheppard et al 1999; Sheppard et al 2004; Ettema et al 2006; Sheppard and Miller 2006). There is a very limited finding on local scour depth for wide piers particularly the piers with rectangular shape. The mechanism of local scour at wide pier for different pier shapes is important because it will help engineers to reasonably estimate the local scour. Besides that, data on the equilibrium scour time for different pier shapes is still lacking, available laboratory data is not sufficient and limited to circular pier shape only. Example of the studies conducted on circular pier was presented by Ettema 1980; Graf 1995; Melville and Chiew 1999. In addition, investigation related to the formation of scour holes and sedimentary structures are relevant to a variety of scientific disciplines, including hydraulic engineering, fluid mechanics, oceanography and geomorphology. Engineering research up to now has concentrated on flow fields around bridge pier (e.g. Dey, 1995; Kirkil et al., 2008; Ettema et al., 2006), but none of these were aimed at investigating the formation of frontal scour holes and downstream deposition. In fact, investigations on formation of scour structures between different pier shapes especially for wide piers are also limited.

[1]Ph.D Candidate, Water Resources Engineering, Dept. of Civil Engineering, Faculty of Engineering, Univ. Putra Malaysia. (corresponding author).
[2] Professor, Dept. of Civil Engineering, Faculty of Engineering, Univ. Putra Malaysia.
[3]Professor, Dept. of Civil Engineering, Faculty of Engineering, Univ. Pertahanan Nasional Malaysia.
[4]Senior Lecturer, Dept. of Civil Engineering, Faculty of Engineering, Univ. Putra Malaysia.

Therefore, the primary objectives of this study were to show the effect of wide pier shape, pier size, uniform bed cohesionless sediment, equilibrium time (t_e) and the scour mechanism of frontal scour hole and sedimentary structures on equilibrium local scour depth (d_{se}). Besides that, the evaluation of existing methodologies for predicting maximum local scour depth at wide piers also presented.

Experimental Setup

20 experiments were conducted in a rectangular glass and bricksided flume, 50 m long, 1.5 m wide and 2.0 m deep, located at the hydraulic laboratory of the National Hydraulic Research Institute of Malaysia, (NAHRIM) in Kuala Lumpur, Malaysia. Two types of pier shapes (circular and rectangular) were tested. The total numbers of tested piers from each shape are five and the total numbers of piers for both shapes are ten. Each type of piers shape has same pier width, 0.060, 0.076, 0.102, 0.140 and 0.165 m. Cohesionless uniform sediments were used as bed material with median particle size, d_{50} = 0.23 mm and d_{50} = 0.80 mm, while the geometric standard deviation, σ_g = 1.3 and σ_g = 1.26 for the first sediment type and second sediment type respectively. In the brick sided part of the flume, a working section in the form of a recess with 10 m long was filled with uniform sediment up to 0.4 m depth. The location of sand bed recess is about 13.5 m downstream of flume inlet and the pier model was installed in the middle of sediment section about 17.5 m downstream the flume inlet. Single pier models were fixed at the center of the flume width. A 60kW centrifugal variable speed pumps supplied 0.14 m^3/s of flow rate through 250 mm diameter pipe to the flume. A valve at the pipeline is used to control the discharge and the water is supplied by pumping system at upstream of the flume. Calibration of the pump was conducted with measuring flow rates and percentage of valve opening. Before each experiment, the sand bed was leveled and the flume carefully filled with water so as not to disturb the planar bed.

The flow depth was maintained at 0.25 m for all of the experiments. Flow-velocity readings were measured using an area velocity module (AVM) that was located on the streambed, upstream from the experimental area. A vertical point gauge with 0.1 mm precision on the Vernier scale was used to measure scour depth. Besides, there is a carriage where can be moved along the flume wall for the measuring the water depth in the flume. Critical shear velocity, U^*_c, and critical flow velocity, U_c, for sediment entrainment, were determined based on expressions given in Melville and Coleman (2000). The experiments were performed under clear-water conditions at threshold flow intensity $V/V_c \approx 0.95$, i.e., the flow intensity inducing maximum local scour depth, in which V is average approach flow velocity. In order to get smooth flow transition, ramps located at the beginning and ending of the sand bed recess was constructed with slope 1: 5 (vertical: horizontal). The ramps can be clearly seen in Fig. 1.

The process of local scour at bridge piers is time dependent. Equilibrium between the erosive capability of the flow and the resistance to motion of the bed materials is progressively attained through erosion of the flow boundary. In fine-grained materials (sands and gravels), the equilibrium or final depth of local scour d_{se} is rapidly attained in live-bed conditions, but rather more slowly in clear-water conditions (Melville & Chiew, 1999). Thus, the experiments were continued until the equilibrium local scour depth recorded where the rate of change in the scour depth was become insignificant or does not exceed 5% of the pier diameter in the succeeding 24 hours period (Melville and Chiew, 1999). Scour depth measurements were purposely taken at interval of 10 minute for 6 times, followed by readings at interval of 30 minutes for 4 times and for every 1 hour for 24 hours or more. Fig. 2 shows the pictures of circular and rectangular pier during experiment and after 24hr runtime.

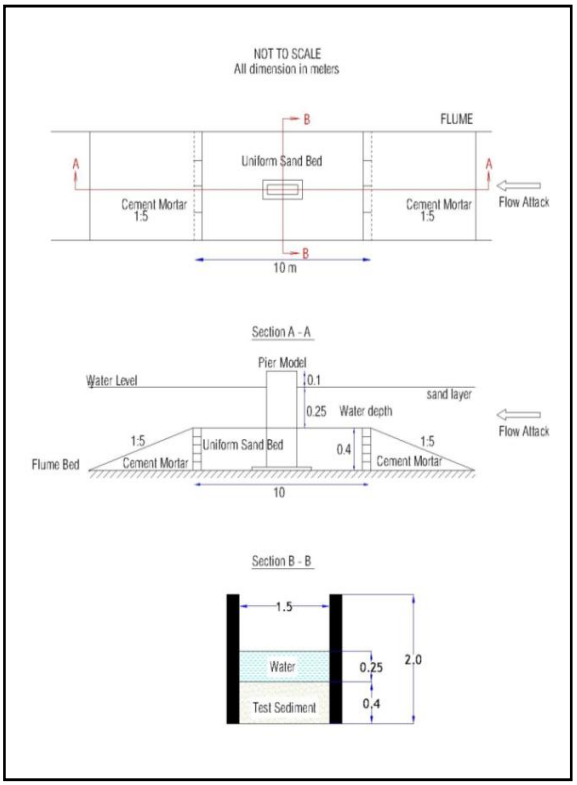

Fig. 1. Schematic Drawing for Experimental Setup

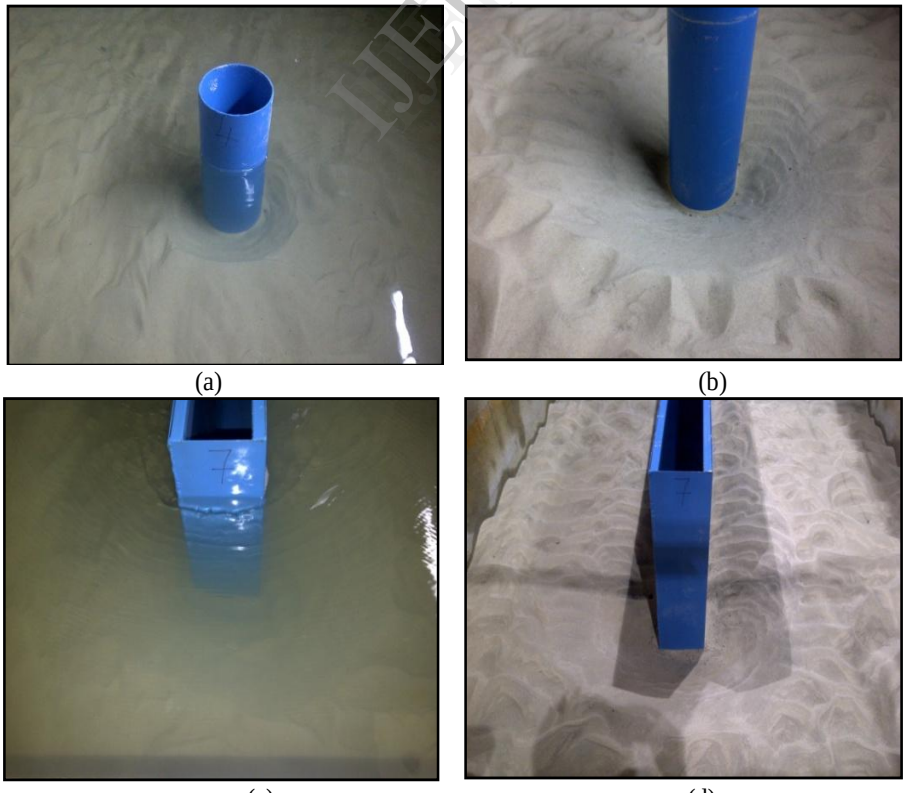

Fig. 2. The local scour depth during experiment and post-experiment for b = 140 mm; (a) circular pier ; (b) scour depth result after achieved equilibrium time (view from upstream) (c) rectangular pier (d) scour depth result after achieved equilibrium time (view from upstream)

Experimental Results

The pier width, sediment and flow variables for the 20 experiments are given in Table 1 along with test durations and computed structure, sediment and flow dimensionless parameters. The scour depths for each type of pier were demonstrated in Fig. 3. The pattern shows logic fact where the greater values of pier size give deeper value of scour depth.

Table 1. Experimental Data

Run	Pier Width	Sediment		Water Flow			Test duration	Equilibrium Scour depth	Dimensionless parameters				
		d_{50}		Depth	Velocity	Critical Velocity							
	b (m)	(mm)	□	y (m)	V (m/s)	V_c (m/s)	(h)	d_{se} (m)	y/b	V/Vc	b/d_{50}	dse/b	Sh
1	0.165	0.23	1.30	0.25	0.27	0.285	23	0.197	1.52	0.95	717	1.19	C
2	0.140	0.23	1.30	0.25	0.27	0.285	23	0.167	1.79	0.95	609	1.19	C
3	0.102	0.23	1.30	0.25	0.27	0.285	22	0.125	2.45	0.95	443	1.23	C
4	0.076	0.23	1.30	0.25	0.27	0.285	22	0.106	3.29	0.95	330	1.39	C
5	0.060	0.23	1.30	0.25	0.27	0.285	13	0.071	4.17	0.95	261	1.18	C
6	0.165	0.80	1.26	0.25	0.27	0.285	18	0.182	1.52	0.95	206	1.10	C
7	0.140	0.80	1.26	0.25	0.27	0.285	20	0.133	1.79	0.95	175	0.95	C
8	0.102	0.80	1.26	0.25	0.27	0.285	19	0.116	2.45	0.95	128	1.14	C
9	0.076	0.80	1.26	0.25	0.27	0.285	17	0.073	3.29	0.95	95	0.96	C
10	0.060	0.80	1.26	0.25	0.27	0.285	13	0.065	4.17	0.95	75	1.08	C
11	0.165	0.23	1.30	0.25	0.36	0.380	21	0.209	1.52	0.95	717	1.27	R
12	0.140	0.23	1.30	0.25	0.36	0.380	20	0.159	1.79	0.95	609	1.14	R
13	0.102	0.23	1.30	0.25	0.36	0.380	20	0.129	2.45	0.95	443	1.27	R
14	0.076	0.23	1.30	0.25	0.36	0.380	20	0.102	3.29	0.95	330	1.34	R
15	0.060	0.23	1.30	0.25	0.36	0.380	13	0.072	4.17	0.95	261	1.21	R
16	0.165	0.80	1.26	0.25	0.36	0.380	25	0.198	1.52	0.95	206	1.20	R
17	0.140	0.80	1.26	0.25	0.36	0.380	21	0.150	1.79	0.95	175	1.07	R
18	0.102	0.80	1.26	0.25	0.36	0.380	21	0.120	2.45	0.95	128	1.17	R
19	0.076	0.80	1.26	0.25	0.36	0.380	20	0.085	3.29	0.95	95	1.12	R
20	0.060	0.80	1.26	0.25	0.36	0.380	14	0.073	4.17	0.95	75	1.22	R

Sh = pier shape

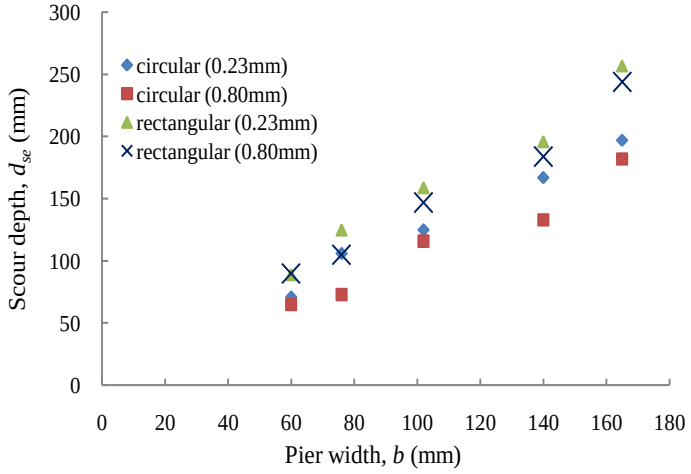

Fig. 3. Results of scour depth for each type of pier in different uniform cohesionless sediment

Influence of Sediment Coarseness

The effect of sediment coarseness, b/d_{50} is strongly concerned in the lack of agreement between measurement of pier scour in the field and predictions of scour depths based on formulas which is derived from laboratory data. Ettema (1980) explained, for smaller values of ratio of pier width to sediment size, individual grains are large relative to the groove excavated by the downflow and erosion is impeded. This is because the porous bed dissipates some of the energy of the downflow. Recent study demonstrates significant scour depth reductions for increasing b/d_{50} (Sheppard *et al*., 2004). In this part, the influence of sediment coarseness, b/d_{50} between wide pier shape, pier size and two types of uniform bed cohesionless sediment on equilibrium local scour depth for twenty experiments are presented.

The influence of b/d_{50} on local scour depth is showed in y/b groups. The wide pier problem is usually considered to be a concern when the relative depth, y/b, is too small to allow the vortices to fully develop. Earlier investigation of the dependence of scour depth on y/b with small piles and very small water depths is presented by Ettema (1980). Sheppard et al (1999) were carried out tests with the large piers indicates that the threshold y/b should be closer to 2. However, most researchers would associate the wide pier problem with relative depths around 1.0 (Jones & Sheppard, 2000). In this study, the flow depth is maintained whereas the pier width is varied. Four groups of y/b (0-1, 1-2, 2-3 and > 3) were calculated to demonstrate the effect of sediment coarseness on scour depth. To illustrate the functional dependence of d_{se}/b on b/d_{50}, all of the 20 data points are plotted in Fig 4. All values of d_{se}/b were corrected with several factors related to the effects of pier shape and flow depth ratio which as presented by Melville and Sutherland (1988). Laboratory data from the literature (Ettema, 1980; Ettema et al., 1998; Sheppard et al., 2004; Lee and Sturm 2009) have been added to Fig. 4 in order to show more detailed trends and a wider range of applicability. Most of the laboratory data in the range of b/d_{50} = 143 – 4155 are from the clear water scour experiments of Sheppard et al (2004). The range of ratios of b/d_{50} from this study was from 75 to 717 and the d_{se}/b values are within 0.95 – 1.39.

In Fig. 4, these plots clearly show the reduced dependence of d_{se}/b on b/d_{50} with increased values of on b/d_{50}. The trend for smaller values of b/d_{50} is similar to that reported by several other investigators, while the trend when the d_{se}/b is reduced on b/d_{50} is one of the particular interests for some researchers (Sheppard et al., 2004; Lee & Sturm, 2009). By the points in this study, it was proved that for large values of b/d_{50}, the values of d_{se}/b become reduced. Furthermore, it was verify the functional dependence of normalized scour depth d_{se}/b on b/d_{50} in the clear-water scour range reported earlier by Sheppard et al (1995); Jones and Sheppard (2000) and Sheppard et al (2004). The data in this graph were divided into two groups where the peak value was occurred at b/d_{50} = 25 where it is recorded from data of Lee & Sturm (2009). All data in Fig 4. are well represented by the following equation:

$$\frac{d_{se}}{b} = -0.004\left(\frac{b}{d_{50}}\right)^2 + 0.252\frac{b}{d_{50}} - 0.149 \qquad 4 \le b/d_{50} \le 25 \qquad (1)$$

$$\frac{d_{se}}{b} = \frac{2}{\left(0.027\frac{b}{d_{50}} - 0.6\right)^{1.4} + 1.3} + 1.8\ , \qquad 25 \le b/d_{50} \le 1 \text{ x } 10^4 \qquad (2)$$

which is plotted as upper envelope in the same figure.

From Sheppard et al (2004), the reason for the reduction in scour depth is suspected that it is due to the suspended sediment induced reduction in bed shear stress. This is because this reduction in shear stress is almost due to a reduced degree of turbulence in the flow because of the presence of suspended sediment (Sheppard et al., 2004). This situation also happened for some experiments in this study especially when the water level in the reservoir is low, the sediment in that reservoir causes water to become turbid. This sensitivity was not known in the beginning of the experiments. From the observation, it would takes eight to nine hours to get the turbidity of the water became low. However, suspended sediment concentrations were very low for most of the experiments. In this regard, that might be one reason why the points in this results is scatter and slightly lower from different researchers.

Nevertheless, another reason why the values of d_{se}/b become reduced is demonstrated by Lee & Sturm, (2009). They were recorded the instantaneous velocities near the nose of the pier to show that the pier scouring mechanism is related to the large–scale unsteadiness of the primary horseshoe vortex. They were found that the quasiperiodic oscillation of the horseshoe vortex is related to transport of sediment particles during the scouring process and the ratio of the vertical turbulence intensity to the rms value of the phase-averaged streamwise velocity was a constant. By postulating that these two measures of turbulence velocity scales are related to the two time scales of lifting and transport of sediment particles, they were concluded that the time-scale ratio (or frequency ratio) essentially reflected by the value of b/d_{50}.

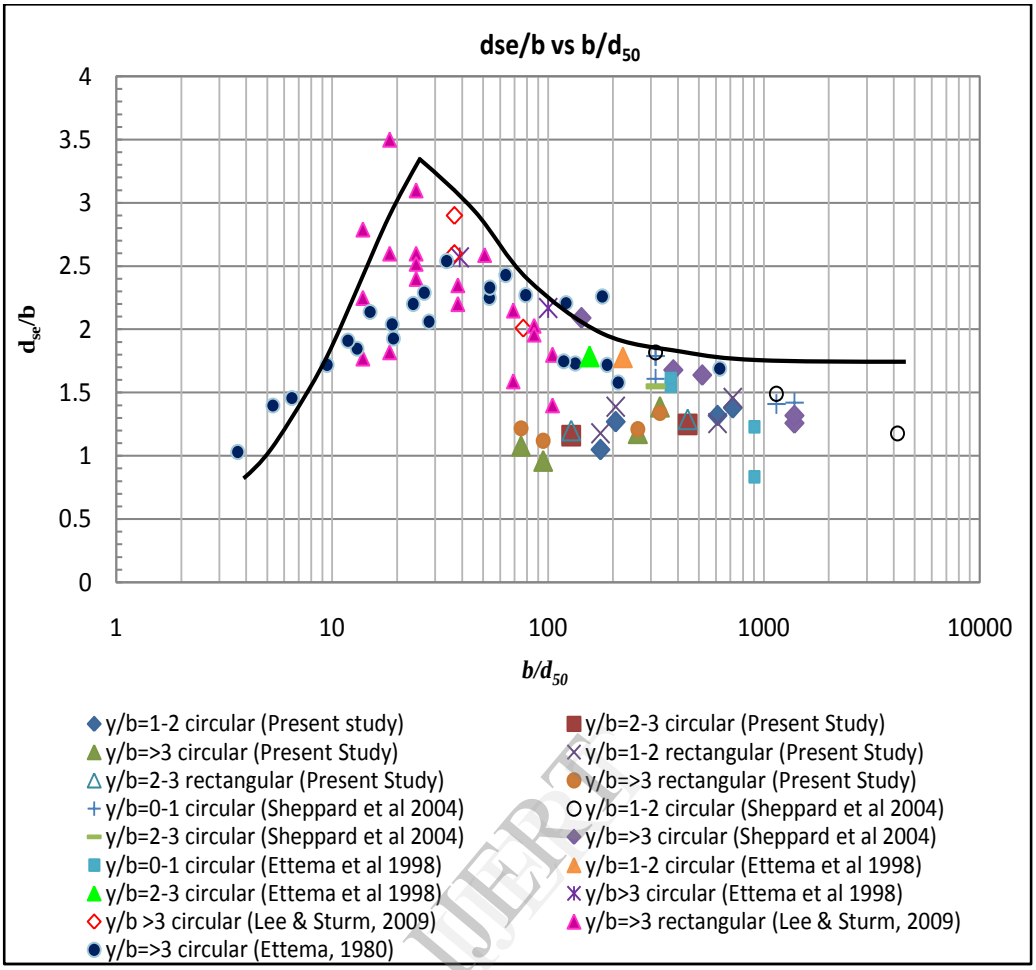

Fig. 4 Effect of d_{se}/b on b/d_{50}

Influence of Equilibrium Time on Pier Scour Depth

In order to clarify the effect of time on the development of scour depth at circular and rectangular piers under clear water conditions, the result for 20 experiments with different pier width and two types of uniform bed cohesionless sediment are presented. Fig. 5 shows the new data for the temporal development of the scour hole plotted for d_s/d_{se} versus t/t_e, with the sediment coarseness as a third parameter. In this plot, d_{se} represents the scour depth at a particular time, t while t_e is time for equilibrium depth. It shows a group of curves with value of sediment coarseness ranges from 75 – 717 for different type of sediments and pier shapes. The data indicate that 50% of the equilibrium scour depth is achieved in a varies of time which is from 0.7% - 11% of t_e, according to the sediment coarseness values. As well, 80% of the equilibrium scour depth developed in a time varying from 10% to almost 70% of the time equilibrium. The data depict the significance of time in estimation of scour depth.

The data in Fig. 5 also can be represented by the following equation:

$$\frac{d_s}{d_{se}} = exp\left\{-0.03\left|\frac{1}{0.95}ln\left(\frac{t}{t_e}\right)\right|^{1.6}\right\} \qquad (3)$$

where it is plotted in Fig. 6 and represent as upper limit curve or general equation for all the data. The modulus sign in (3) is require to ensure that the exponential function is negative.

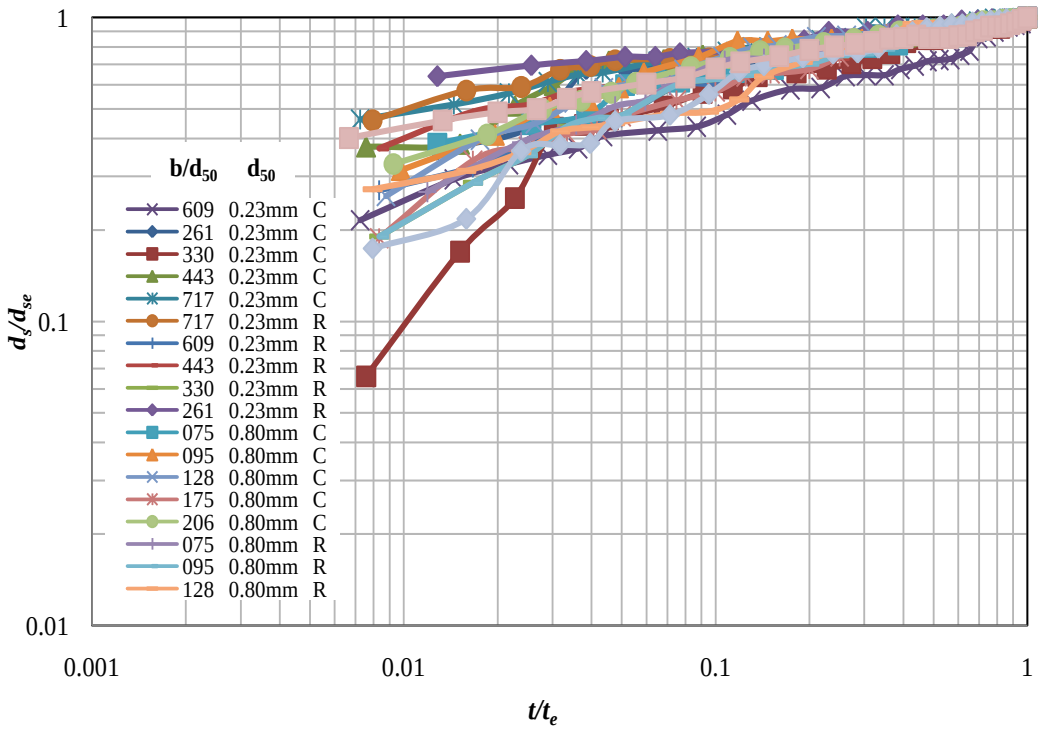

Fig. 5. New laboratory Data Showing Temporal Development of Scour Depth

The effects of flow shallowness in this experiment are depicted in Fig. 7. The data are plotted with different pier shapes and sediment sizes. The flow depth, y is constant while the pier width, b are varied. The term equilibrium time scale, t^* was used to demonstrate the trend of flow shallowness. The method in determining of t^* is according to Melville and Chiew (1999) where t^* can be expressed as:

$$t^* = \frac{Vt_e}{b} \tag{4}$$

From Fig. 7, it is indicate that t_e is depend on flow shallowness for lower values of y/b and this is verify the relationship between scour depth and flow shallowness as shown by Melville and Coleman (2000); Melville (2008); Ettema (1980) and Melville and Chiew (1999) where t_e and d_{se} are inherently interdependent and the trend should have similar dependence on the same set of parameters. Therefore, the result for wide piers in this study seems to be consistent with the observations of those researchers. In terms of shape, the equilibrium time scale, t^* for rectangular data in coarse sediment (d_{50}=0.80mm) demonstrate the highest value compared to the others. This is logic where the greater sediment size used, the higher the value of velocity (V) is needed to get maximum pier scour depth, d_{se} and thus make the t^* value increased.

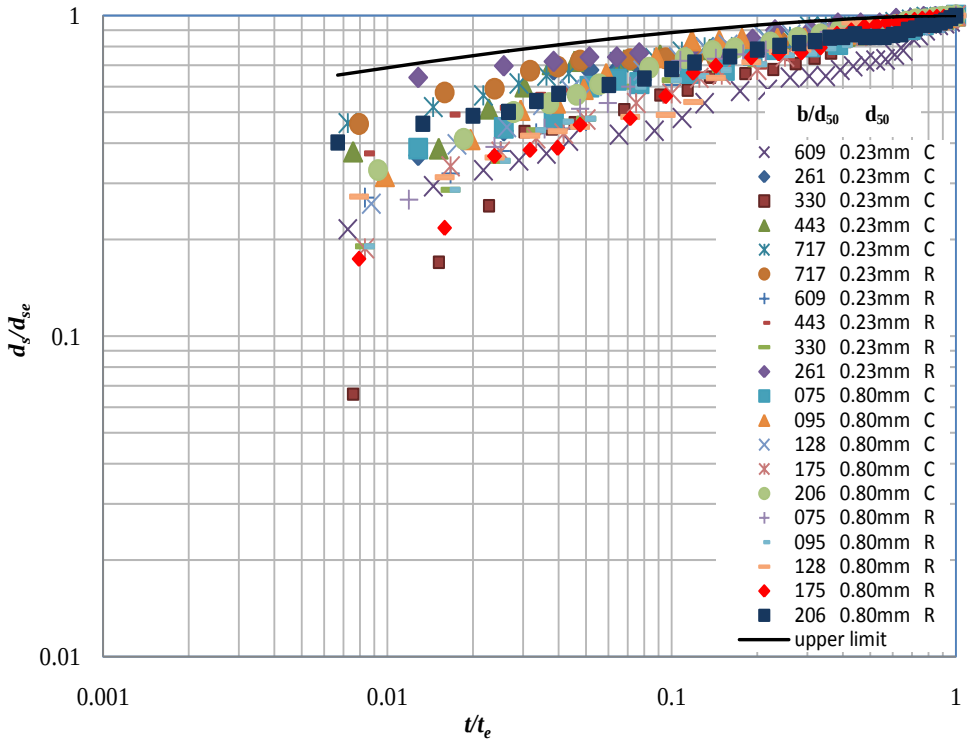

Fig. 6. Plot of Eq. (3) Indicating Temporal Development of Local Scour Depth for Flow Intensity V/V_c=0.95

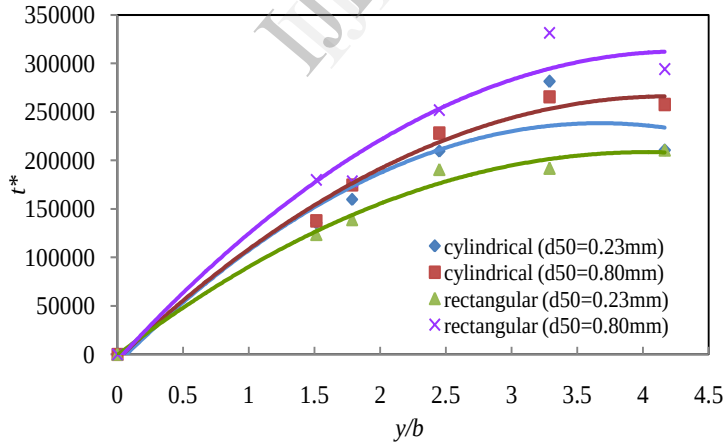

Fig. 7. New laboratory Data of Wide Piers Showing Relation Between t^* and y/b

Scour Mechanism

Relationship between Frontal Scour Holes and Sediment Ridge

This part shows the effect of wide pier shapes on frontal scour holes and sediment ridge from both of uniform cohesionless bed sediments. The volumes of scoured and deposited material for each experiment were calculated from the distance of length (l), width(w) and height (h) of scour holes and sediment ridge. Fig. 8 shows the distance for each variable in determination of scoured and deposited volumes in scour contours which is created in *Surfer*. In this context, the volumes are computed with scour depth multiplied by scour width and length. Also, same calculation is used for sediment ridge

volume. Fig 9 shows the relationship between normalized $V_{rectangular}/V_{circular}$ on pier width, (b) at frontal scour holes and sediment ridge for d_{50}=0.23 mm and 0.80 mm. All patterns depict that the $V_{rectangular}/V_{circular}$ are depend on b.

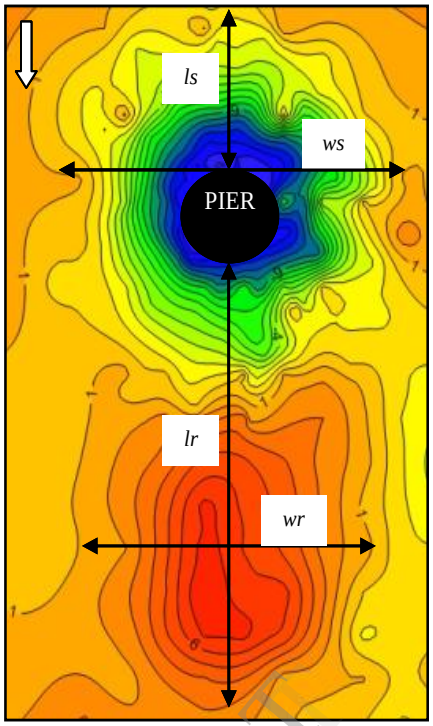

Fig.8. Scour depth contour and locations of frontal scour holes and sediment ridge variables, indicated by arrows. (*ls*=scour hole length; *ws*=scour hole width; *lr*=ridge length; and *wr*=ridge width. The white arrow indicates the direction of flow. Picture is not to scale).

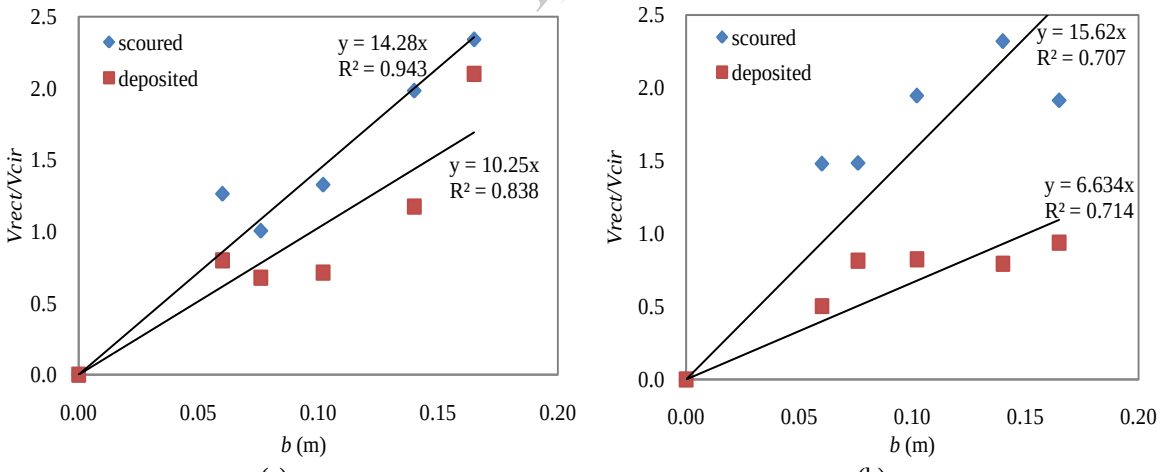

Fig. 9. Linear relationship between normalized $V_{rectangular}/V_{circular}$ and pier width, b for scoured and deposited in different sediment sizes; (a) d_{50} = 0.23 mm and (b) d_{50} = 0.80 mm

Next, Fig. 10 shows result from the volume calculation on the basis of the grid-files created in *Surfer*. Correlating pier width, b with normalized between volume calculated using *Surfer* and volume of actual scour depth (*hlw*) shows a clear linear relationship for all pier shapes and sediment sizes (Fig. 8 (a), (b), (c) and (d)). In this context, the volumes which are calculated with *Surfer* are predicted values (V_{cir} and V_{rec}) while *hlw* is the measured values. Comparing scoured and deposited volumes, it is indicated that all of deposited values are lower than scoured values. It might be due to some of the sediment particles were transported by the water flow due to the effect of turbulence flow in scour hole area. Fig. 10 can

be graphically shows in Fig. 11 where all of the plots are combined. By doing this, a significant (linear) relationship with pier width, b was achieved where these plots can be represented by the following equations

$$\frac{V_{predicted}}{hlw} = 6.707b \tag{5}$$

$$\frac{V_{predicted}}{hlw} = 4.654b \tag{6}$$

where (5) is for scoured and (6) is from deposited data points. In this regard, there is clear relation between frontal scour holes and sediment ridge where the volume amount whether scoured or deposited are depend on the pier size. Therefore, the influences of pier size, flow, sediment size and pier scour factor on the distance of scour width, (w_s) and scour length (l_s), at piers can be expressed functionally as

$$w_s, l_s = f\left(b, \frac{b}{d_{50}}, \frac{y}{b}, k_s, k_y\right) \tag{7}$$

in which b = pier width; b/d_{50} = sediment coarseness; y/b = flow shallowness; k_s = pier shape factor; and k_y = flow depth factor. Since the tests used equilibrium time, uniform sediment and zero skew angles, thus k_t, k_σ and k_θ are equal to 1.

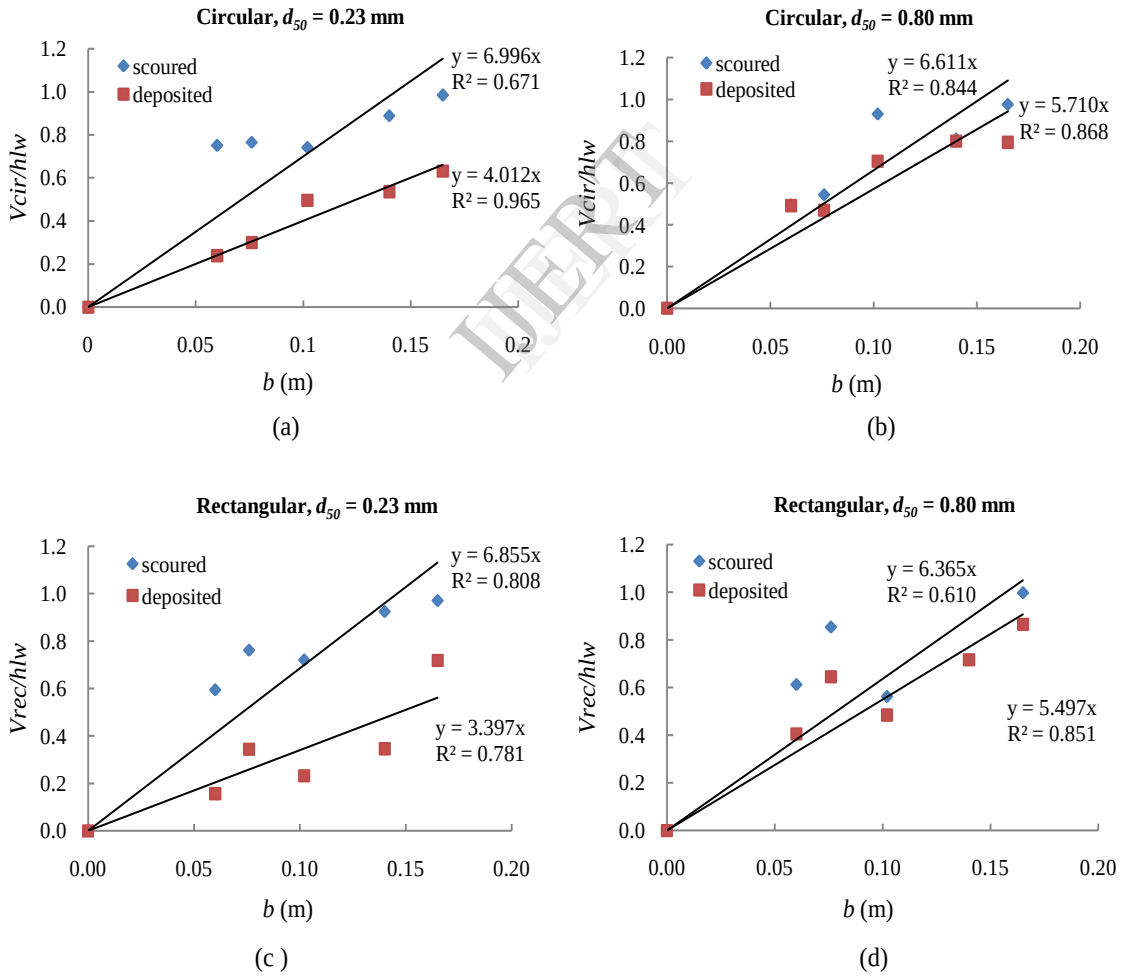

Fig. 10. Effect of normalized $V_{predicted}/V_{measured}$ *(hlw)* on b for different pier shapes and sediment sizes; (a) circular, d_{50}=0.23 mm; (b) circular, d_{50}=0.80; (c) rectangular, d_{50}=0.23; and (d) rectangular, d_{50}=0.80.

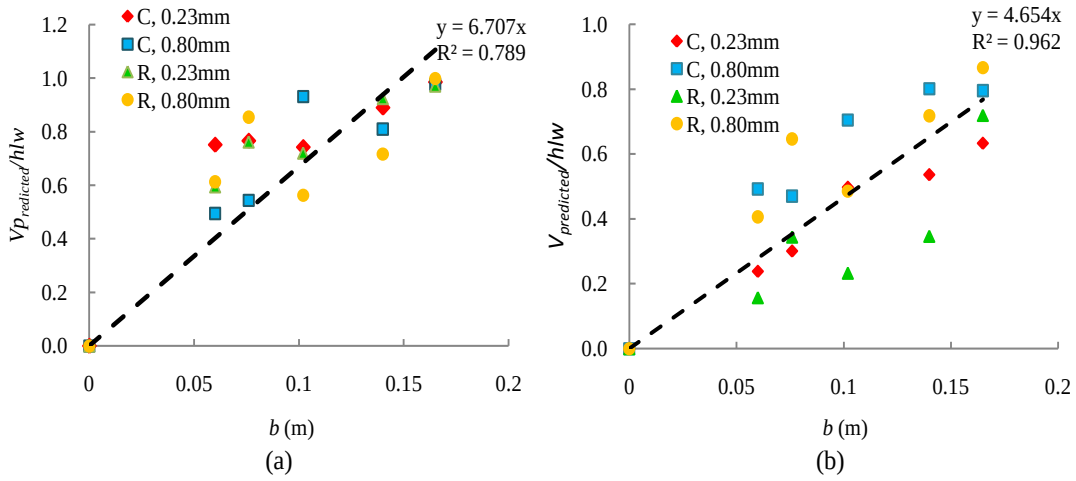

Fig 11. Normalized $V_{predicted}/V_{measured}$ *(hlw)* with *b* for (a) scoured; and (b) deposited

Evaluation of Existing Methodologies for Predicting Maximum Local Scour Depth at Wide Piers

Fig. 12 shows a comparison between predicted scour depth using four existing empirical methods: Hydraulic Engineering Circular No. 18, HEC-18 (Arneson et al 2012); Jones and Sheppard (2000); Sheppard and Miller (2006); and Sheppard and Melville (2011). All of the methods were based on wide pier scour estimation. These plots show the d_{se}/b for predicted values were ranges from 0.36 to 2.40 whilst the d_{se}/b for measured values was from 0.95 to 1.39. Data from Jones and Sheppard (2000) show a good agreement and close to the measured values while data from Sheppard & Miller (2006) and HEC-18 (Arneson, 2012) just slightly higher than the Jones and Sheppard (2000). Sheppard and Melville (2011) depict that the points are just upper than Sheppard & Miller (2006) data. However, values from Johnson (1999) shows under predicted data points.

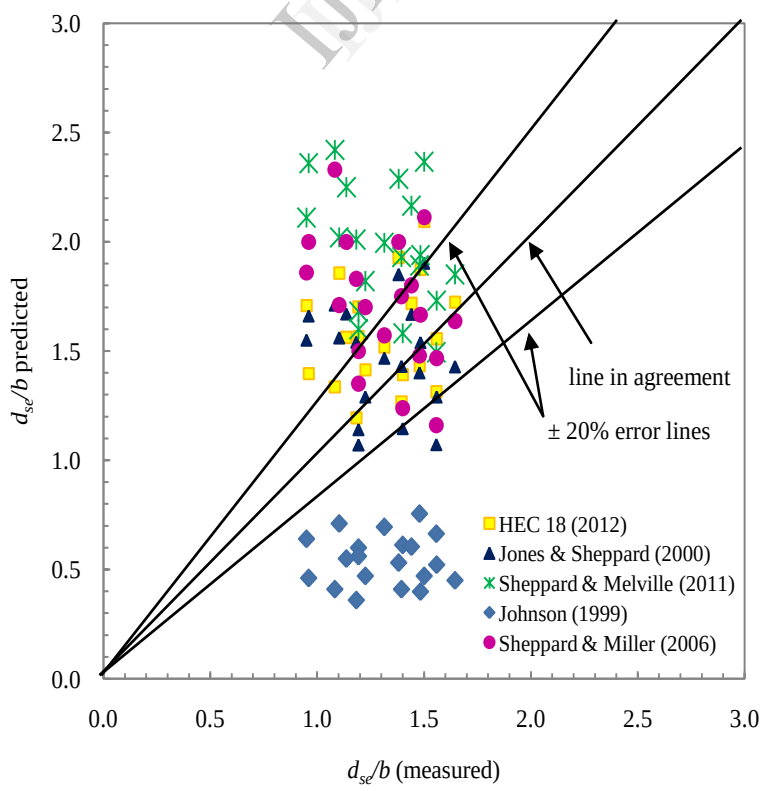

Fig. 12. Comparison of existing methodologies for predicting maximum local scour depth

Conclusions

In conclusion, the effect of local scour depth at wide piers configuration on sediment coarseness, time equilibrium and scour mechanism between frontal scour and sediment ridge were investigated. From analysis of data in this study, it was found that the relative scour depth d_{se}/b decreased with the increasing values of sediment coarseness b/d_{50}. Two continuous upper envelope equations for pier scour depth as a function of b/d_{50} were developed according to the value of b/d_{50} (≤ 25 and > 25). The maximum value of d_{se}/b occurred at a value of $b/d_{50} \approx 25$ as reported by other investigators. For large values of b/d_{50}, the d_{se}/b decreased in agreement with experiments in very large flumes as well as with the three data points from the previous researchers. The temporal development of local scour depth with new laboratory data is demonstrated for flow intensity $V/V_c = 0.95$. The data verify that the equilibrium depth of scour at a wide pier under clear-water conditions is approached asymptotically as shown in Fig. 5 and the data can be represented in eq. (3). Next, correlation between volumes of frontal scour holes and sediment ridge with pier width is revealed and leads to a very significant (linear) relationship with pier sizes. The relations for scoured and deposited are given in eq. (5) and (6). Recommended functions for the effects of pier size, flow, sediment size and pier scour factor on the scour width, (w_s) and scour length (l_s), also can be express functionally in eq. (7). The evaluation of existing methodologies for predicting maximum local scour depth at wide piers shows the empirical equation from Jones and Sheppard (2000) demonstrate a good agreement with measured values in this study. Overall, the validation of experimental results and analysis of the effects of pier width, pier shape, bed sediment size and equilibrium time on scour depth verifies the theory of wide piers for the most part. However, the results of the present study are limited to clear-water conditions, steady flow, non-cohesive sediments and subcritical flow conditions. An important practical limitation with laboratory experiments on pier configuration is flume width; the size of the flume is not wide enough to facilitate scour experiments for large values of b.

Acknowledgements

The financial support from the Research University Grant Scheme (RUGS) given by University Putra Malaysia (Grant No. 05-01-10-0904RU) for this project is acknowledged. The experiments were conducted in the Hydraulic Laboratory in National Hydraulic Research Institute of Malaysia (NAHRIM).

References

Arneson, L. A., Zevenbergen, L. W., Lagasse, P. F. and Clopper, P.E. (2012). "Evaluating scour at bridges." Hydraulic Engineering Circular No. 18 (HEC-18). Rep. No. FHWA-HIF-12-003, Federal Highway Administration,Washington, DC.

Dey, S., Bose, S. K., and Sastry, G. L. N. (1995). "Clear-water scour at circular piers: A model." J. Hydraul. Eng., 121(12), 869–876.

Ettema, R. (1980). "Scour around bridge piers." *Rep. No. 216*, Univ. of Auckland, Auckland, New Zealand.

Ettema, R., Melville, B. W., and Brian, B. (1998). "Scale effect in pier-scour experiment." *Journal of Hydraulic Engineering–ASCE*, 124(6), 639–642.

Ettema, R., Kirkil, G., and Muste, M. _2006_. "Similitude of large-scale turbulence in experiments on local scour at cylinders." *J. Hydraul.Eng.*, 132_1_, 33–40.

Garde, R. J. and Kothyari, U.C. (1998). Scour Around Bridge Piers. PINSA 64, A, No. 4, July 1998, pp 569-580

Graf, W. H. (1995). ''Local scour around piers.'' *Annu. Rep.*, Laboratoire de Recherches Hydrauliques, Ecole Polytechnique Federale de Lausanne, Lausanne, Switzerland, B.33.1–B.33.8.

Johnson, Peggy A.(1999), .Scour at Wide Piers Relative to Flow Depth,. Stream Stability and Scour at Highway Bridges, Compendium of ASCE conference papers edited by E. V. Richardson and P. F. Lagasse, pp280 . 287,.

Johnson , P.A., and Torrico, E. F., 1994. Scour Around wide Piers in Shallow Water. Transportation research record 1471, 66-70.

Jones, J. and Sheppard, D. (2000) Scour at Wide Bridge Pier. Building Partnerships: pp. 1-10.

Kirkil, G., Constantinescu, S.G., Ettema, R., 2008. Coherent structures in the flow field around a circular cylinder with scour hole. Journal of Hydraulic Engineering 134, 572–587.

Lee, O. S. and Sturm, T. W. (2009). "Effect of Sediment Size Scaling on Physical Modeling of Bridge Pier Scour." *Journal of Hydraulic Engineering–ASCE*, 135(10), 793–802.

Melville, B. W (2008). The Physics of Local Scour at Bridge Piers. Fourth International Conference on Scour and Erosion. ISCE-4. 5-7th November, 2008. Tokyo, Japan.

Melville, B. W., and Chiew, Y. M. (1999). "Time scale for local scour at bridge piers." *J. Hydraul. Eng.*, 125(1) 59–65.

Melville, B.W. and Coleman, S.E. (2000). *Bridge Scour*. Water Resources Publications,LLC, Colorado, U.S.A., 550 p.

Melville, B. W., and Sutherland, A. J. (1988). "Design method for local scour at bridge piers." *J. Hydraul. Eng.*, 114(10), 1210–1226.

Sheppard, D. M., and Miller, W. (2006). "Live-bed local pier scour experiments." *Journal of Hydraulic Engineering–ASCE*, 132(7), 635–642.

Sheppard, D. M, and Melville. B. W. (2011). Scour at wide piers and long skewed piers. Report (National Cooperative Highway Research Program) ; 682. Washington, D.C. : Transportation Research Board, 2011

Sheppard, D. M., Odeh, M., and Glasser, T. (2004). "Large scale clear-water local pier scour experiments." *Journal of Hydraulic Engineering–ASCE*, 130(10), 957–963.

Sheppard, D. M., Ontowirjo, B., and Zhao, G. (1995). "Local scour near single piles in steady currents." *Proc., 1st Hydraulics Engineering Conf.*, San Antonio.

Sheppard, D. M., Ontowirjo, B., and Zhao, G., (1999). "Conditions of maximum local scour." *Proc., Stream Stability and Scour at HighwayBridges, Resources Engineering Conf. 1991–1998*, E. V. Richardson and P. F. Lagasse, eds., ASCE, Reston, Va.